TUBULAR ANODES WITH HIDDEN CATALYST CONCEPT AND THEIR H_2 TRANSPORT

Luis Antônio Waack Bambace, bambace@dem.inpe.br
Alfredo José Alvim de Castro, ajcastro@ipen.br
Instituto Nacional de Pesquisas Espaciais-INPE. Av. Astronautas 1758. São José dos Campos. CEP 12201-970
Instituto de Pesquisas Energéticas e Nucleares. IPEN Av. Prof. Lineu Prestes, n.2242 São Paulo CEP 05508-000

Abstract. *This paper describes a new kind of fuel cell anode. Templating of microfiber fabrics allows the production of micrometer diameter tubes. Porous wall tubes material may be impregnated with ionomer, if its gelling mixture and solvents have surface energy smaller than the porous wall material. Radiolitic catalyst deposition on impregnated fabrics tubes outer surfaces creates high ionomer-catalyst interface areas. Hydrogen permeable metal shells in contact with catalyst delivers this reagent to catalyst grains, and surface diffusion spreads it over the entire grain surface. The fast evolution in the last 10 years of ionic liquids electroplating, turned it possible to plate Nb/V over such fabrics at room temperature. The large surface area of 10 to 16 μm outer diameter electrodes tubes with around 0.4 mm thickness, allows for negligible H_2 pressure differences in shells of 100 to 300 nm thickness even in high power electrodes. Bipolar plate, micro-flanges and proper opposite tube ends sealing isolate the fuel supply cavity from the rest of the cell. Adaption of some aspects of electronic nanometer via filling CEACs technique assures low porosity tube walls, and therefore effective O_2 and CO blocking as will be shown by the mathematical model in this paper.*

Keywords*: Fuel cell, anode, poisoning free, tubular*

1. INTRODUCTION

There is a lot of investment in tubular reformers, mostly using Palladium, a noble metal, as hydrogen filtering material, once this metal is inert and permeable to H_2. Some metals have H_2 permeability that grows with temperature increase as Pd, others with permeability that decrease in hotter environment as V and Nb, being the latter the most permeable metal to H_2, and more proper to cell usage, due to its lower operation temperature. Once CO poisoning is the major difficulty in using H_2 of on board fuel reformers in fuel cell, low cost cell tubular design not sensible to CO content would allow fuel cells to reach new application markets. Micro-tubular arrangements are able to do so and also to eliminate PEM membranes, but not the use of ionomers. This paper discusses the operation of a patent pending fuel cell anodes made with microfiber fabrics as templates for tubular structures of porous walls with less than 300 nm compact outer layer of Nb or V and external diameter in the 10 to 16 mm range. If the cell tolerates large levels of CO, the reformer is simplified, as it does not have to perform filtering function, and its catalyst does not have strong requirements on CO chemical equilibrium levels, enabling more material to be used as catalyst in the reformer.

2. CELL SET UP AND PRODUCTION PROCESSES

The use of either one of the polymers, copper or alumina μm-fiber fabrics as removable templates, and either tensoactive intermediated pulsed electroplating or chemical vapor deposition techniques, Ledoux et al. (2005), Antunes et al. (2006), Cheek et al. (1999), Vermilyea (1957) and Bambace et al. (2008), porous wall tubes of internal and external diameters in the 6-12 μm and 10-16 μm ranges, respectively, were manufactured. The structures were filled with ionomer, catalyst and finally received a hydrogen (H) permeable shell layer. Some materials are known to have low electrical resistance and good hydrogen transport properties, such as solubility and diffusion. Particularly, the permeability which is the product of solubility by the diffusion coefficient is the crucial property to the determination of H transport through a shell. Niobium (Nb), Vanadium (V) and Tantalum (Ta) have not only the highest hydrogen permeability, but also permeability that increases as colder as it is the environment. Palladium (Pd) has lower permeability when compared with the materials mentioned above, but with values that increase with temperature. Iron (Fe) and nickel (Ni) come next with similar behavior. Exact values of permeability of these last two metals depend on the type of the crystal structure and also of the grain size, as interstitial transport is much higher than by diffusion through the grain body. H contents in metals, in general, are proportional to the square root of the pressure, while H content in some polymers is linearly proportional to the pressure. Carbon is not amongst the best H_2 permeable material, but as carbon nm-tubes have very thin walls and as they are hollow, their H_2 transport was evaluated. The main sources of permeability data are references: Doylei et al. (1995), Zajec and Nemanic (2006), Akamatsua et al. (2005), Sedano et al. (1998), Edwards (1957), Kazarinov (2005), Kocha et al. (2006) and Choi (2004). The most important data for 1 atm H_2 pressure and operation between 60 and 120^{o}C are in the tables 1 and 2. The basic dirty H_2 cell set up is shown in Fig. 1 to Fig. 5. Cathode tubes have uniform catalyst load in its porous walls. Ledoux ECN tubes density is over twice the ECN tubes values, and getting higher densities is the main ECN process goal presently. Air flow in the cell is like air flow in a car air filter. Radiolytic chromium deposition in Ni-NSF followed by hot Cr diffusion, and 1200^{o}C nitrating assures tube walls material is inert, chemically similar to the Los Alamos laboratory bipolar plated material

obtained by nitrating directly plated NiCr alloys (Brady et al. 2004). A description of radiolytic process for catalysts deposition is presented in Silva et al. (2005), and this process is used to apply metal catalyst over tubes impregnation layers.

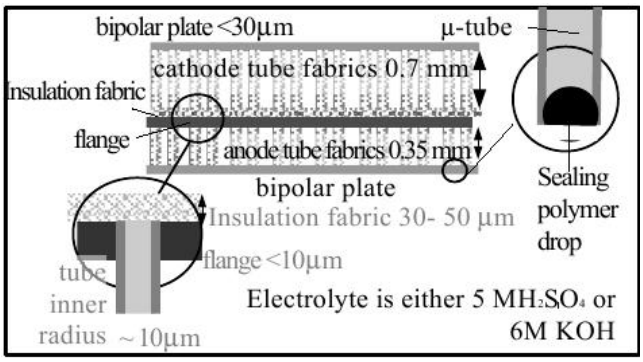

Figure 1. Typical cell lateral cross section

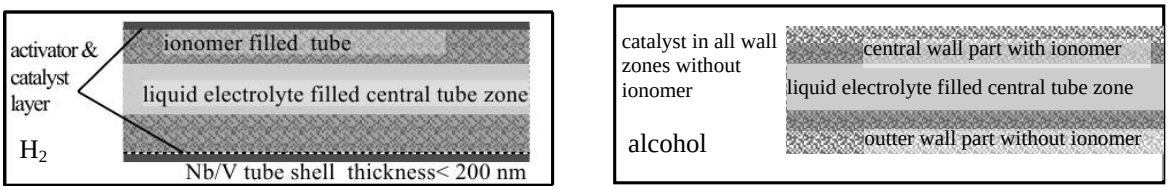

Figure 2. H_2 and alcohol anode tubes cross sections

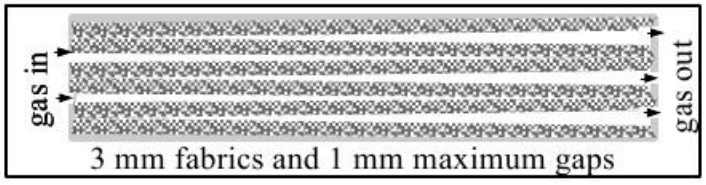

Figure 3. Anode & cathode top view with gas flow scheme

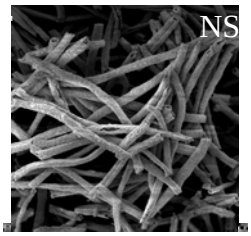

Figure 4. SEM Images of Nano Structured Metal Foam, (NSF), 5 µm inner radius & 70-100 nm foam cell elements

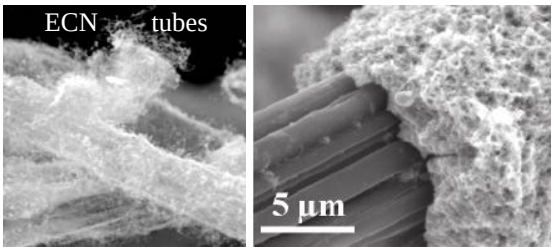

Figure 5. SEM Images of tubes of Entangled Carbon Nanotubes walls, (ECN), and Ledoux ECN covered carbon fiber

As surface tension is the energy needed to form a unit area of a specific interface, if the gelling volume of a polymer solvent solution that wets a porous walls set is exactly this set volume, it will fill only these walls, in order to minimize total surface energy. If it is smaller, only the tubes central zone will be filled. Melting and solidifying slowly the polymer reduces porosity. Nickel boride layers building over the NSF is also an alternative way for protection. Direct building of

NSF with NiCr alloys showed itself too difficult and expensive. ECN tubes were also manufactured. Fortunately, partially burned material like metal and alumina microfiber fabrics are also good substrates to ECN growing. Metal and some partially burned materials allow diffusion of the catalyst, reducing the nm-tubes quantity to a given amount of catalyst. Different working gases needs different temperatures and metals cannot be used with all gases. Adopted techniques were the ones of Ledoux et al. (2005) and Antunes et al. (2006). Many metals that in the past required hot fused salt electroplating may now be plated at room temperature with ionic liquids like the imidazolium chloride, amides and organic sulfur compounds. Furthermore, Nb was one of the first metals deposited with its chlorides, imidazolium chloride, and $AlCl_3$ as optional compound to better ionic conductivity (Cheek et al. 1999). After testing this patent protected process, we seek another path; specially, we used a bath of vanadium chloride and a euthetic mix of CH_3-H_2S-CH_3, C_2H_5-H_2S-C_2H_5. Fabric surface impregnation with metal chlorides increases the growing rate of metal in the direction parallel to the support surface, as well as it reduces porosity. Gelling of H_2 impermeable polymer solution drops at tubes tips, seals it, and if this is done before filtering metal is applied the barrier it is more efficient. But before doing so, it is needed to build the flanges, doing a temporary tip sealing with the same method. Tips sealed, for instance with acrylic, may be pressed towards a tyxothropic mix of polymer, its specific solvent and colloidal silica, or such silica and its preparation suspension emulsions. After cure, a rotating sand paper set up removed excess of polymer and the tip protection is dissolved with specific solvent by ultrasonic cleaning. Possible room temperature cure polymers are high melting temperature PVC, Poly(4-methyl pentene-1) and Poly(vinyl fluoride) among others. Carded fabrics with fiber normal to bipolar plates have the shortest ionic path, but available fabrics are thin, and assembly with many fabrics shall be used. Entangled Poly (acrylonitrile) fabrics with most of the fibers with a low angle with a chosen direction are available for carbon fiber fabrics production, and are thicker and easier to handle. The process crack effects in cells are open issues. The main ECN problem is electric current transfer between the nm-tubes that may be increased by building graphite bonding among them. This process is under development. The more aligned the nm-tubes are to a line normal to the template fiber axis, the electron leakage is larger. This is not a problem in anodes due to the H_2 permeable V/Nb film conductivity.

3. MATERIAL AND METHODS

To calculate the H and CO mass fluxes it is necessary to use some “flux resistances” in analogy with thermal or real electric resistances. The first one is the H transport resistance by diffusion in the shell (R_{SH}), associated with inner (R_{OH}), and outer (R_{IH}), interface resistances, related to the release and capture of H_2 by the surfaces. Due to the low dependence of thermal contact resistance with the thickness, a constriction resistance ($R_{CONST-H}$), equal to half of the contact resistance model cited in Cooper et all (1969), describes additional resistance to H flux toward catalyst grains. It is assumed that H_2 adsorbed at a cylindrical surface, goes to a spherical particle, with half of it in the ionomer and half of it in the metal wall, and an internal catalyst particle resistance (R_{CIH}) is added in series with the latter two. There are pores in the shell, due to random catalyst and electroplating activation particles positions and random aspects of the structure and due to its small size neither an integer number of V/Nb atoms fit in the space, nor it is possible to overcome non homogeneity by structural deformation. The number of pores is larger than the number of initial particles, and there are some very small pores in the particles, as the inter-atomic distances of different materials do not match. These pores will present either liquid or Knudsen diffusion, if dry. So, many pores in parallel carry either H_2 or CO to the ionomer, with resistances R_{PI-X} (R_{PI-CO}/R_{PI-H}), and resistances related to access of gases through pores to the catalyst particles, R_{PC-X} (R_{PC-H}/R_{PC-CO}) are linked to the single to multiple spots coplanar coupling in a semi-infinite media. R_{ICX} (R_{ICCO}/R_{ICH}) are internal resistances of particle to gases coming from these pores to the catalyst-ionomer interfaces. A Cooper constriction resistance ($R_{CONST-O}$) shall be added to O_2. Resistances R_{PI-X} are far larger than diffusion ones in gas or liquid filled pores cases with diameters smaller than 1 nm. In the gas filled case, the Knudsen number based in diameters are very large. In liquid filled cases the pores transition from normal to Knudsen diffusion is considered (Bitter, 1991), but more pores will have a boundary layer of adsorbed molecules and organized molecules attracted by their dipoles that blocks the flux of CO and H_2, so pore effective diameter, d_{PE} is reduced by twice this layer thickness.

$$R_{SH} = (2\,\pi L\, p_{HS})^{-1}\, ln(d_{SHE}/d_{SHI}) \tag{1}$$

$$R_{CONST-X} = 0.25\,\pi^{-1}\, a^{-1}\, (1-a/b)^{3/2}/n \tag{2}$$

$$R_{X-IE} = f_I\,(2\,\pi L\, \tau_I\, p_{XI})^{-1}\, ln(d_{SHI}/d_{TI}) \tag{3}$$

$$R_{PC-X} \sim [\Sigma\, 0.5^{0.5}(d_{PE}^{-1}+b)+d_{ij}^{-1}]/\, p_{XI} \tag{4}$$

In the equations above, p_{HS} is the H permeability of the shell, p_{XI} is the ionomer permeability to the gas X, τ_I is its tortuosity due to presence of the tube porous wall, f_I is the occupation factor of ionomer in the wall, the tube inner, inner shell and outer shell diameters are respectively d_{TI}, d_{SHI} and d_{SHE}; a is ¼ of the average area of a catalyst particle, b is $(4\,S\,n^{-1}\pi^{-1})^{1/2}$,

for n the number of particles and S the area, d_{ij} are distances from source i to pore j. R_{PC-X} is always larger than real ones if all d_{ij}≡0. Permeability are effective ones, due to the very small thickness of the system components, see Galinski et al. (2006).

Gases that reach the ionomer have a resistance related with its path toward the inner electrolyte, R_{H-IE} ($R_{H-IE}/R_{CO-IE}/R_{O-IE}$) to H/CO/O_2 outward path. If the porous wall support material is a good H transport media, catalyst may be placed on it, and as its H transport is relevant, the corresponding structure may be represented as a fin, with a length larger than the wall thickness to represent the effect of a tortuous path. In all cases some core to surface H_2 flux resistance is assumed. Due to an intrinsic porosity macromolecules have a larger diffusion coefficient than a low permeability metal, a double fin model was tested for H_2 mass transfer and its end transfer to the electrolyte. So:

$$d^2C_i/dx^2-b_{ii}C_i+b_{ij}C_j = 0 \quad (5)$$

Where C_1 and C_2 are base material and ionomer concentrations, $b_{12}=2h/(r_fD_1)$, in which h is the interface transfer coefficient, r_f the equivalent foam/nm-tube fin radius, D_1 the diffusion coefficient, $b_{22}=b_{21}=2h/(r_{io}\ D_2)$, D_2 is the ionomer diffusion coefficient, r_{IO} the equivalent ionomer fin radius; $b_{11}=b_{12}-2i_o[10^{dec}-10^{-dec}]/(r_fD_1)$, i_o is the exchange current, dec is the number of decades of polarization. A bi-quadratic equation gives the exponential ratios. Boundary conditions are insulated tips at liquid and shell interfaces for metal/foam and ionomer fins with knew concentration at shell for both fins. By solving this with actual coupling b_{ij}, ones sees that the wall support material and ionomer are in equilibrium in short distances from the shell, so a single material model with average properties and eventual reaction is used. This gives either a logarithmic field or a I_o Bessel function, where the distance multiplied by $[4f\ i_o10^{dec}/(r_fD_1)]^{0.5}$ is its argument, with f representing the support material volume fraction, I_v to large argument is $e^x(2\pi x)^{-0.5}\{1-(4v^2-1)/(8x)+(4v^2-9)(4v^2-1)/(8x)^2\}$. Due to the presence of internal liquid electrolyte and the small thickness of ionomer tubular layer, it will be assumed that its pores are entirely filled with liquid electrolyte. The carbon nm-tubes typically have 16 nm diameter, and 3 nm wall thickness, so mean free paths are respectively 10 and 6,6 nm for H_2 and CO respectively. The corresponding Knudsen number is nearly one to H_2/H and nearly 2/3 to CO. The surface diffusion is enhanced by free H/H_2 that jumps directly to distant points, and vacuum pipe calculation are valid. The resistances are combined according to the circuit shown in Fig. 1. The CO may be oxidized in the catalyst either reacting with water or with O_2, H_2O_2 or O_2H^+. The Pt catalyst H_2 and CO adsorption kinetic constants are $3.26\cdot10^{-5}$ and, $3.26\cdot10^{-5}$ m/s, desorption constants for H and CO are $3.81\cdot10^{-6}$ and $2.74\cdot10^{-11}$ mol $m^{-1}s^{-1}$, H and CO-OH_{ADS} exchange currents respectively 8 A/m^2 and $1.04\cdot10^{-6}$ A/m^2. CO-O_2 exchange current is near 2.5 times CO-OH_{ADS} one, and H_2O_2-CO even higher. Sieverts ideal solid or Rault models solution kinetics are fast enough to equilibrium concentrations to be considered. If excess ionomer is used, an internal pure layer of it brings an additional logarithmic resistance R_{OLX}.

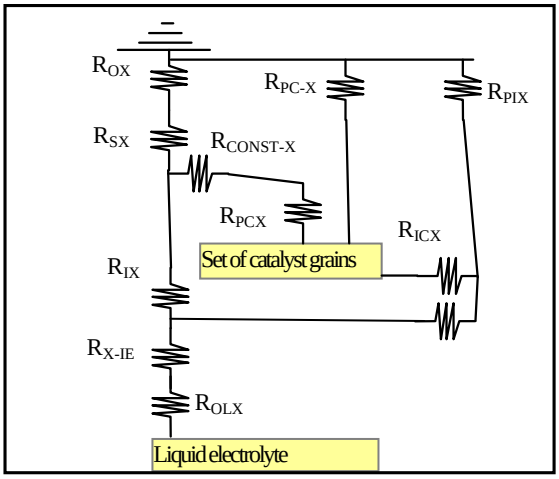

Figure 6. Transport Model, described with resistances.

With this, the tolerance of the new architecture to high levels of CO in the fuel is evaluated as well as the cross flow of gases. Interface area for a given electrode thickness t_e and mean area diameter d_t, and tube fraction f_t in the electrode, the effective area is $4f_t(t_e/d_t)$. Since near the electric insulator one has more reactivity an efficiency factor α shall be used and the effective area is corrected to $4\alpha f_t(t_e/d_t)$. For common PEM cells, there are only small differences in CO and H transfer coefficient to the catalyst due mainly to their different permeability in the liquid present in the electrode. As the ratio between the transfer coefficients of H and CO becomes larger, the cell is less sensitive to CO. Another point in CO tolerance is its consumption, linked to water gas shift in the anode, electrochemical oxidation, O_2 bleeding and eventual H_2O_2 presence. If the shell blocks O_2 the fuel cell bleeding is safer, and despite of cathode consumption electrokinetic flows and small ionomer thickness, some supply of O_2 is allowed to promote CO oxidation.

4. ANODE FILTERING PROPERTIES

The high hydrogen-cover shell interface area and the H transport at 80°C through the shell assure its high concentration at catalyst region such as for Pd, V and Nb shells. Ni shell case is uncertain due to a large variation of literature permeability data, probably related with the higher grain interfacing values. Either in cubic or in hexagonal compact crystals, interstitial H_2/H occurs, but the gaps are very close to H atomic diameter. Diffusion along grain boundaries seems to be the main mode, despite of vacancy, interstitial and crowd-ion mechanisms. CO nickel transport papers confirm that hypothesis. Due to the dense nucleation of the catalyst grains, and auto-catalytic processes employed the system grain size, g_s, range from 1.6 to 3 nm, which is much smaller than any literature measured Ni sample as in [6]. Furthermore, the system operates at higher temperature. Using these results with typical Arrhenius temperature and grain size corrections, a permeability of 3.9×10^{-10} is found. As the available grain contour perimeter per unit of area is proportional to $1/g_s$, permeability for our system is higher. Table 1 gives the equivalent partial H_2 pressure at the catalyst grains to be exposed in a gas environment to produce a flux of H_2 equivalent to the one assured by the set up at operational conditions, using catalyst loads of 0.1 mg-Pt/cm^2-bp or 0.05 mg-Pd/cm^2-bp, where bp indicates that bipolar plate area is the reference. It was noticed that even with very small HER activity porous wall material, with an exchange current i_f of the order of 10^{-6}A/m^2, almost no H_2 reaches internal electrolyte at 2 decades of chemical polarization for Ni foam setup despite the 2 to 3 μm ionomer thickness. This is easily shown with the ratio of $I_1(mx)$ fluxes at the 2 shell positions, calculated with the large argument approximations. For carbon nanotube with diffusive approximation and V foam the exchange current i_f must increase to 5×10^{-4}A/m^2, and is near 8×10^{-5}A/m^2 for effective transition regime in a Monte Carlo analysis. The H content in feed gas may be reduced if the power is smaller. The shell pores are tiny in its inner, and eventually larger at outer layers if the shell is thick enough for defects propagation, or over 15 nm. Minimum low porosity shell thickness is about 16 nm for Ni (electrodeless), 60 nm for Pd, and 160 for ionic liquids electroplated V. As V is a very good H conductor its thickness has minimum value. Thick shells of high H permeability material, blocks more effectively O_2 and CO. This made the natural O_2 bleeding to anode catalyst of the system, to be effectively blocked by the shell, so the feeding H_2 will not mix with O_2. As O_2 access to catalyst is partially blocked by the ionomer and even by the liquid electrolyte, despite of its convective flow, levels are not harmful to catalysis, even if the CO content in feeding mixture is low, and its bleeding high enough to a fast oxidation of the residual CO from dirty mixtures. In the case of 0.35 mm thick anodes, the Ni shell couplings for H_2, CO and O_2 are 0.328, 2.72×10^{-2} and 4.09×10^{-4} mol/m^2-bp/s/atm$^{0.5}$, respectively. This means a strong selectivity in favor to H_2. Palladium shell has an H_2 coupling of 6.9100mol/m^2-bp/s/atm$^{0.5}$. Being thicker, CO and O_2 couplings falls to 9×10^{-3} and 1.4×10^{-4} mol/m^2-bp/s/atm$^{0.5}$. The V shell couplings are 1.88×10^{8}, 3.3×10^{-3} and 4.9×10^{-4} mol/m^2-bp/s/atm$^{0.5}$ for H_2, CO and O_2 respectively. This means that CO and O_2 transfer to H_2 feeding cavity is effectively blocked by this latter shell. Once the fuel cell is turned off, H_2 blocking due to reactions ceases and filled Ni foam coupling with electrolyte becomes 0.16 mol/m^2-bp/s/atm$^{0.5}$, critical for high permeability shells, being necessary to cut H_2 feeding as soon as possible. Corresponding couplings to carbon nm-tubes and vanadium foam are even higher. CO and O_2 couplings are in the range of 8×10^{-5} to 1.2×10^{-4} mol/m2-bp/s/atm$^{0.5}$. At operation, the cell has eletrokinetic convection and levels of O_2 about 0.04mol/m^3 at liquid electrolyte so that some residual O_2 will be available to help CO oxidation, and this kinetic is known to be better than adsorbed OH one.

Table 1. H_2 equivalent contents at catalyst for different shell materials $H_{2FLUX}=K(P_E^{0,5}-P_C^{0,5})$.

Shell material & thickness (nm)	Current (A/m^2)	Sieverts H_2 Pressure loss (Pa)	Electrode thickness (mm)
Ni / 18	18500	50,000	0.35
Ni / 18	50000	95000	0.35
Pd /48	5000	0.2	0.35
Pd / 48	9000	0.4	0.35
V / 300	9000	5^x10^{-4}	0.35

The average chemical polarization needed to produce the above currents, is very low, once the catalyst is plenty of H_2. In the 50000 A/m^2 Ni shell case, the concentration is equal to that of pure water interface with a pressure of 1.86 atm. Notice that more than half of the total catalysts grains area is operating in contact with the ionomer. Reported exchange currents for Pt in water with this equilibrium H_2 content is 10 A/m^2-$Pt_{EXPOSED}$. The current IPEN Pt or Pt-Ru grains diameter, produced by electron beam or radiation reduction in alcohol, is 4 nm, so for 50% of the grain inserted in the shell the catalysis area is 49 m^2. This means less than 1.9 decades of polarization is needed to reach 70000A/m^2-bp, with Buttler-Volmer reaction mechanism this means. Depending on the reaction mechanism, a polarization of only 133 mV is obtained. For other shells the polarization is much smaller. Ionomer ionic resistance is only 270μΩcm/cm^2-bp for an anode with 16 μm external diameter tubes and an interface area to bipolar area ratio of 20 filled with Nafion. Even considering current distribution related losses and use of ionomers with low ionic conductivity and hydrogen permeability, the losses are negligible. For Nafion and 15 A/cm^2-bp, the ionic loss is about 4 mV. In fact, as there is a current distribution where a higher current near fabric electric insulator working as ion bridge, the losses are higher. This is the main reason why less conductive ionomer may be used. An electronic microscope image of one of the tested

structures is shown in Fig. 2. A complete cell setup is shown in Fig. 3. This tube has 10 μm of internal diameter, and it is not filled with ionomer to facilitate the image obtaining. In contact with 5M H_2SO_4, the conductivity of the Nafion will be higher than standard fully hydrated value.

Ni foam has some catalytic activity, but as it is protected against corrosion in acid media with passivation layers of Ni-Cr-N, borides or oxides, with this protection it probably will not have any catalytic activity. Hence a low cost low activity catalyst is employed to avoid H2 cross flow. The closer the catalyst is from the outer wall, the more H2 is available and the more efficient is its use, in this way top catalyst will be placed out of the wall only if there is not enough space on wall inner surface. Possible control catalysts are either organometallic or Ru-sulfides HER catalysts, used not with the purpose of current production but to block H2 flow towards the electrolyte, and to mitigate excessive O2 transport. Arrangements with good H2 penetration, as vanadium foam, offers more catalyst support area, but they have more cross flow problems. This foam showed over 20 times more H transport capacity than carbon nanotubes, due to the strong wall iteration of the latter. This and other tested geometries are the result of new nanotechnology and electrochemical processes in fuel cell design (Galinski et al. 2006).

5. CONCLUSION

This study shows that tubular fabric anode systems with proper design are promising anodes for future high power fuels cells. Niobium, Vanadium and Palladium shells allow proper H_2 flux, while effectively blocking CO and O_2. On the other hand, with nickel, it is not possible to assure a high enough hydrogen flux without further tests and CO/H_2 blocking will be not enough to assure working with any CO content. How the permeability varies with the grain size reduction remains an open question, and that is the main question for Ni. As Nb/V/Pd shells block the O_2 flux to fuel supply cavity, the small flux of O_2 in the ionomer helps the oxidation of any CO passing trough the shell. When the cell is operating at full power, H_2 that does not react in the main catalyst layer is oxidized in the porous wall matrix filled with ionomer. When the cell H_2 crossing is about 0.16mol/m^2-bp/s, implying in the need of immediate cut of its H_2 supply.

6. REFERENCES

Akamatsua,T., Kumea,Y., Komiyaa, K., Yukawaa, H., Morinagaa, M. and Yamaguchib, S., 2005, "Electrochemical method for measuring hydrogen permeability through metals", Journal of Alloys and Compounds, Vol. 393, pp. 302–306.

Antunes, E.F., Lobo, A.O., Corat E.J., Trava-Airoldi,V.J., Martin; A.A. and Verıssimo, C., 2006, "Comparative study of 1st and 2nd order Raman spectra of MWCNT at visible and infrared laser excitation", Carbon, Vol. 44, pp. 2202-2211.

Bambace, L.A.W., Castro, A.J.A., Favalli, R.C., Ramos, F. and Villanova, H.F., 2008, "Tubular Anodes with Hidden Catalyst Concept and their Hydrogen Transport", Proceedings of WREC X World Renewable Energy Congress, Vol.1, Glasgow. Scotland.

Brady ,M.P., Weisbrod, K., Paulauskas, I., Buchanan, R.A., More, K.L., Wang, H., Wilson, M., Garzon, F. and Walker, L.R. 2004, "Protection of Metallic Bipolar Plates in PEM Fuel Cells", Scripta Materialia, Vol. 50, pp. 1017-22.

Bitter, J.G.A., 1991, "Transport Mechanisms in Membrane Separation Processes", Plenum Publishing Corporation, NY.ISBN 0-306-43849-6, 470 p.

Cheek, H.C., Long, H.C. and Trulove, P.C., 1999, "Electrodeposition of Niobium and Tantalum from a room temperature molten salt system", Proceedings of International Symposium (12th) on Molten Salts and the 1999 Joint International Meeting, Vol. 1, Honolulu, Hawaii.

Choi, P., 2004, "Investigation of Thermodynamic and Transport Properties of Proton-Exchange Membranes in Fuel Cell Applications", Worcester Polytechnic Institute. PhD Thesis.

Cooper, M. G., Mikic, B. B. and Yovanovich, M. M., 1969, "Thermal Contact Conductance", Journal of Heat Mass Transfer, Vol. 12, pp. 279-300.

Doylei, D. M., Palumbo, G., Aust K. T., El-Sherik, A. M. and Erb, U., 1995, Acta metall, mater., Vol. 43, No. 8, pp. 3027-3033.

Edwards, A. G., 1957, "Measurement of the diffusion rate of hydrogen in nickel", British Journal of Applied Physics, Vol. 406, No.8, pp.406-409.

Galinski, M., Lewandowski, A. and Stepniak, I.,2006. "Ionic liquids as electrolytes", Electrochimica Acta, Vol. 51,. pp. 5567-5580.

Kazarinov, R.F., 2005, "Thin-film, Solid-state Proton Exchange Membranes for Fuel Cells", Bell Labs.

Kocha,S.S; Yang, J.D and Yi, J.S., 2006, "Characterization of Gas Crossover and Its Implications in PEM Fuel Cells", AIChE Journal, Vol. 52, No. 5, pp.1916-1925.

Ledoux, MJ., Gulino,G., Vieira R., Amadoua, J., Nguyena, P., Galvagno, S., Centi, G. and Pham-Huua, C., 2005, "C_2H_6 as an active carbon source for a large scale synthesis of carbon nanotubes by chemical vapour deposition", Applied Catalysis A: General, Vol. 279, pp. 89-97.

Sedano,L.A., Alberici, S., Perujo,A., Camposilvan, J. and Douglas, K., 1998, "Derivation of hydrogen transport parameters in carbon fibre composites by modelling transient release in isovolumetric desorption experiments", Journal of Nuclear Materials, Vol. 258-263, pp. 662-665.

Silva, DF., Spinace, E.V., Oliveira Neto, A., Pino, ES. and Cruz, V.A., 2005, "Processo de preparação de eletrocatalisadores utilizando processos radiolíticos para aplicação em células a combustível com membrana trocadora de prótons", PI0505416-8.
Vermilyea, D.A., 1957, "Electrodeposition on Metal Whiskers", The Journal of Chemical Physics Vol. 27, pp. 814-815.
Zajec,B and Nemanic,V., 2006, "Determination of parameters in surface limited hydrogen permeation through metal membrane", Journal of Membrane Science, Vol. 280, pp. 335–342.

7. RESPONSIBILITY NOTICE

The authors are the only responsible for the printed material included in this paper.